LETTER IEICE Electronics Express, Vol.14, No.3, 1–9

Non-contact physiological signal monitoring system based on Doppler radar

Long Chen[a)], **Xining Yang, Jianfeng Wu, and Lingyan Fan**
School of Electronic Information, Hangzhou Dianzi University, No. 1, 2nd Avenue Xiasha District, Hangzhou City, 310018, China
a) *chenlong@hdu.edu.cn*

Abstract: A non-contact physiological signal monitoring system was proposed using Doppler radar sensor to detect the movement of human thoracic cavity. The system consists of Doppler radar sensor, signal conditioning, MCU data processing and wireless communication. The system collects human chest movement due to heart and respiration (pleura fretting signals for conditioning). The experimental results show that the Doppler radar that the system used with the zero phase IIR digital filter can achieve real-time monitoring, store the physiological data, separate respiration and heartbeat signals, eliminate the distortion of the signal phase and have advantages of small size, low power consumption, strong penetration.

Keywords: Doppler radar sensor, digital filter, physiological signal monitoring

Classification: Circuits and modules for electronic instrumentation

References

[1] J. C. Lin: "Microwave sensing of physiological movement and volume change: a review," Bioelectromagnetics **13** (1992) 557 (DOI: 10.1002/bem.2250130610).
[2] C. Gu: "Short-range noncontact sensors for healthcare and other emerging applications: a review," Sensors **16** (2016) 1169 (DOI: 10.3390/s16081169).
[3] A. D. Droitcour, *et al.*: "Signal-to-noise ratio in Doppler radar system for heart and respiratory rate measurements," IEEE Trans. Microw. Theory Techn. **57** (2009) 2498 (DOI: 10.1109/TMTT.2009.2029668).
[4] O. Daisuke, *et al.*: "Human sensing technique using microwave Doppler radar based on higher-order local auto-correlation features," IEICE Tech. Rep. **113** (2013) 13 EA2013-3, SIP2013-3, SP2013-3.
[5] J. Wo, *et al.*: "Noninvasive respiration movement sensor based on distributed Bragg reflector fiber laser with beat frequency interrogation," J. Biomed. Opt. **19** (2014) 017003 (DOI: 10.1117/1.JBO.19.1.017003).
[6] J. H. Lee and S. O. Park: "A 14 GHz non-contact radar system for long range heart rate detection," Antennas & Propagation (ISAP) **1** (2013) 204.
[7] Y. S. Lee, *et al.*: "Monitoring and analysis of respiratory patterns using microwave Doppler radar," IEEE J. Transl. Eng. Health Med. **31** (2014) 1800912. eCollection (DOI: 10.1109/JTEHM.2014.2365776).
[8] H. Li and P. Zhang: "Fast design of active filter based on MATLAB and EDA," Int. Conf. Signal Processing Systems **3** (2010) 693 (DOI: 10.1109/ICSPS.2010.5555760).

DOI: 10.1587/elex.14.20161178
Received November 28, 2016
Accepted December 16, 2016
Publicized January 18, 2017
Copyedited February 10, 2017

IEICE Electronics Express, Vol.14, No.3, 1–9

[9] D. Qiao, *et al.*: "Non-contact physiological signal detection using continuous wave Doppler radar," Biomed. Mater. Eng. **24** (2014) 993 (DOI: 10.3233/BME-130896).
[10] C. Charalambous and M. M. Saleh: "Design of zero-phase spherically symmetric N-dimensional IIR digital filters," IEE Proc. G **139** (2002) 419 (DOI: 10.1049/ip-g-2.1992.0068).
[11] G. A. Lampropoulos, *et al.*: "A two-step design of 2-D zero-phase IIR filters," IEEE Conf. Decision and Control **25** (1986) 10 (DOI: 10.1109/CDC.1986.267449).

1 Introduction

Physiological parameters (such as respiration, heartbeat signals) are important indexes for modern medical detection. Monitoring of physiological parameters can provide a reliable basis of diagnosis and treatment for doctors. Contact monitoring devices are most commonly used in the hospitals. These devices directly connect to patients using wearable sensors, bands or electrodes in order to achieve the physiological signal monitoring. These methods have the advantages of high signal quality and low noise. However, the detection processes normally impact on patient's psychological or physical constraints. Sometime, the methods can not accurately reflect the physiological changes, mainly due to complex installation of electrodes and difficult operation. Doppler radar sensors can pass through specific materials, such as cloth, silk etc. to detect human physiological signals. The systems overcome the shortcomings of traditional physiological monitoring system, with advantages of non-contact, remote monitoring and simple [1]. Therefore, it has been more and more attention in the fields of clinical medicine, health care and many other applications [2].

The aim of this paper is to design an analog and digital filters for a Doppler radar signal acquisition system to separate physiological signals. The experimental results show that the use of a zero phase IIR filter can accurately extract heartbeat and respiration signals without distortion in physiological conditions, guarantee signal integrity, increase accuracy and reliability of the detection.

2 The basic system components and working principle

The block diagram of non-contact Doppler radar system for physiological signal monitoring is shown in Fig. 1. It comprises a signal processing module, amplifying and filtering modules, level move, A/D conversion, MCU data processing modules and wireless communication module. Since signals detected by Doppler radar sensor have small amplitude with low signal to noise ratio [3], the multiple amplifier filters were designed to improve the signal to noise ratio as well as lifting signal to an acceptable level by MCU. Our system uses 2.4G wireless RF modules communicating with PC, the PC displays and stores information of respiration and heartbeat in a real-time manner.

The principle of Doppler radar sensor for detecting human chest movement is that there is a phase shift between the radar transmitting and receiving signals, and

DOI: 10.1587/elex.14.20161178
Received November 28, 2016
Accepted December 16, 2016
Publicized January 18, 2017
Copyedited February 10, 2017

IEICE Electronics Express, Vol.14, No.3, 1–9

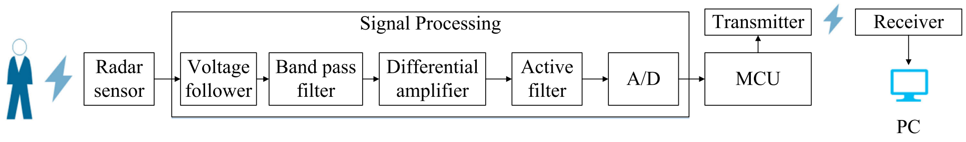

Fig. 1. The block diagram of system for monitoring respiration and heartbeat signal

the amount of phase shift is proportional to the changes of chest position. For monitoring respiration and heartbeat application (as shown in Fig. 2), the Doppler radar system transmits a continuous-wave (CW) signal to human chest, and then receives a signal similar to the transmitted signal with its phase modulated by the chest position. The information related to the heartbeat and respiration can be extracted by demodulating the phase signal [4].

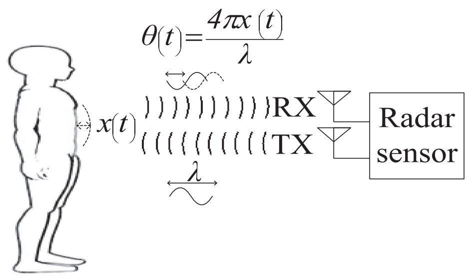

Fig. 2. Experimental setup of the system to detect human chest expansion

It is now assumed that the radar transmit signal $T(t)$ is:

$$T(t) = cos[2\pi f_0 t + \Phi(t)] \tag{1}$$

Where f_0 the signal frequency of radar is transmit, $\Phi(t)$ is phase noise.

The chest movement amplitude is $x(t)$, the distance from radar sensor to the human body is d_0, the distance from emitted radar signals to the chest wall is $d(t) = d_0 + x(t)$, The movement of the chest wall and the transmission of the signal is occurred at the same time, the distance from the radar antenna to the chest wall is at the time of the launch is $d(t - (d(t))/c)$, so the delay time for a round trip is $t_d = \frac{2d\left(t - \frac{d(t)}{c}\right)}{c}$. Since pleura motion cycle $T \gg \frac{d_0}{c}$, the signal received by the radar modulated $R(t)$ is

$$R(t) = cos[2\pi f_0(t - t_d) + \Phi(t - t_d) + \theta_0] \tag{2}$$

Among equation (2) θ_0 is the constant phase shift, it is affected by the phase shift of the target reflection surface, and the delay between the antenna and the mixer. Substitute t_d into equation (2), the received signal is

$$R(t) = cos\left[2\pi f_0 t - \frac{4\pi d_0}{\lambda} - \frac{4\pi x\left(t - \frac{d(t)}{c}\right)}{\lambda} + \Phi\left(t - \frac{2d_0}{c} - \frac{2x\left(t - \frac{d(t)}{c}\right)}{c}\right) + \theta_0\right] \tag{3}$$

DOI: 10.1587/elex.14.20161178
Received November 28, 2016
Accepted December 16, 2016
Publicized January 18, 2017
Copyedited February 10, 2017

Among equation (3) wavelength is $\lambda = c/f_0$. The $(d(t))/c$ in $x(t-(d(t))/c)$, due to the period of thoracic motion $T \gg d_0/c$, so, can be ignored, in the phase noise, $x(t) \ll d_0$, so $2x(t-(d(t))/c)/c$ can be ignored therefor, the received signal can be approximately equal to:

$$R(t) \approx cos\left[2\pi f_0 t - \frac{4\pi d_0}{\lambda} - \frac{4\pi x(t)}{\lambda} + \Phi\left(t - \frac{2d_0}{c}\right) + \theta_0\right] \tag{4}$$

If the signal is multiplied by a $L(t)$ signal which from the same source signal, the target information of this periodic movement can be easily decoded. The phase noise of the received signal is correlated with the $L(t)$, ignore the transformation of the magnitude, $L(t)$ can be described as

$$L(t) = cos(2\pi f_0 t + \Phi(t)) \tag{5}$$

Mixing the received signals and LO signals, and pass through the low pass filter, outputted base-band signal is

$$B(t) = cos\left[\frac{4\pi x(t)}{\lambda} + \Delta\Phi(t) + \theta_1\right] \tag{6}$$

Where $\Delta\Phi(t)$ is the residual phase noise, $\theta_1 = \frac{4\pi d_0}{\lambda} - \theta_0$ is pitch shift by the distance between radar and human body. When θ is $\frac{\pi}{2}$ an odd multiple, $x(t) \ll \lambda$ available

$$B(t) \approx \frac{4\pi x(t)}{\lambda} + \Delta\Phi(t) \tag{7}$$

From equation (7), we can obtained that pleura displacement $x(t)$ and the base-band output is linear. Test shows, the range of body surface vibration caused by respiration was 4–12 mm, body surface vibration amplitude caused by heart rate less than 0.6 mm, when the radar operating frequency is 2–24 GHz, the wavelength range is 1.25 cm–15 cm [5]. Combined with radar resolution, capacity of penetrate obstacles, size and power consumption, the system selected the 10.525 GHz Doppler radar sensor for the physiological monitoring.

3 Circuit design of system hardware

3.1 Circuit design of front-end processing for radar echo signal

Fig. 3 shows a front-end processing circuit of radar echo signal, which comprises a voltage follower and a passive filter. Amplitude variation range from output of

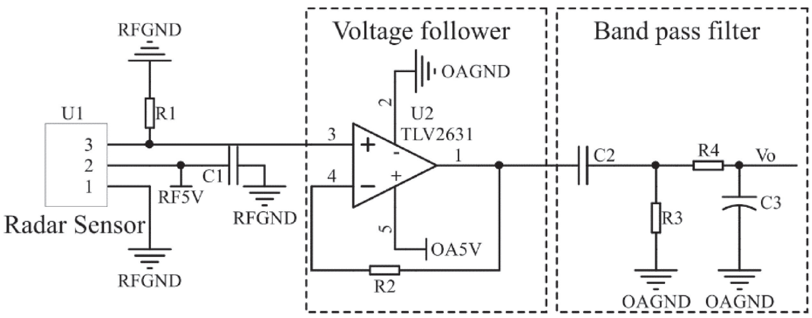

Fig. 3. Front-end processing circuit of radar echo signal

DOI: 10.1587/elex.14.20161178
Received November 28, 2016
Accepted December 16, 2016
Publicized January 18, 2017
Copyedited February 10, 2017

Doppler radar sensor by chest micro movement is 1–20 mV. It shows low amplitude, noise and low load capacity. In order to prevent the DC component leading to saturation of the amplifier, the system uses a passive filter to filter out the DC component, eliminate the effects and enhance the driving capability.

3.2 Designing active band-pass filter

Frequency ranges of normal respiration and heartbeat are 0.2–0.5 Hz and 0.83–3.3 Hz respectively, both of them are very close to the DC signal [6, 7]. This system chose a Butterworth 0.1–10 Hz band-pass filter, which characterizes flat curve of a band-pass amplitude-frequency and slow transition zone. It can achieve better signal filtering and smaller signal attenuation, removing respiration and heartbeat noise obtained by Doppler radar. In order to shorten the transition zone, filter out frequency interference and improve the filter attenuation gain [8], the system used a fourth-order Butterworth low-pass filter and a second-order Butterworth high-pass filter to form a band-pass filter. The Butterworth band-pass filter circuit is shown in Fig. 4.

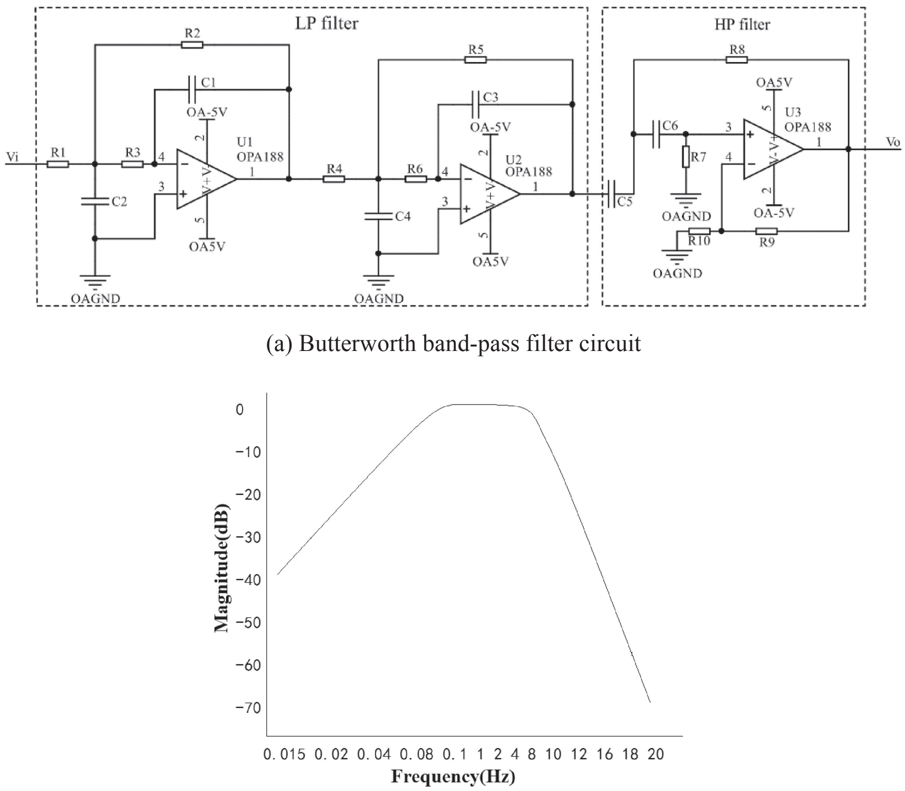

(a) Butterworth band-pass filter circuit

(b) Frequency response of the Butterworth filter

Fig. 4. Circuit and Frequency response of Butterworth band-pass filter

Fig. 4(a) on the left is a four-order low-pass (LP) filter, which contains two multiple feedback (MFB) circuit two-order low-pass filters. For a single second order multiple feedback (MFB) low-pass filter, according to Kirchhoff's theorem and the negative feedback op amps feature, the following parameters can be obtained as equation (8–10):

DOI: 10.1587/elex.14.20161178
Received November 28, 2016
Accepted December 16, 2016
Publicized January 18, 2017
Copyedited February 10, 2017

ELectronics
EXpress
IEICE Electronics Express, Vol.14, No.3, 1–9

$$C\omega_c^2 = \frac{1}{R_2 R_3 C_1 C_2} \tag{8}$$

$$B\omega_c = \frac{1}{C_2}\left(\frac{1}{R_1} + \frac{1}{R_2} + \frac{1}{R_3}\right) \tag{9}$$

$$K = \frac{R_2}{R_1} \tag{10}$$

Where K is the filter gain, ω_c is the filter cutoff frequency, B and C are normalization coefficients. According to an infinite gain multi feedback circuit topology, the obtained normalization coefficient $B = 1.414$, $C = 1$, approximately $10/f_c$ by the rule of thumb is selected C_2. From the cut-off frequency $f_c = 10\,\text{Hz}$ can obtain $C_2 = 1\,\text{uF}$, the filter gains is 1 and 10 respectively. The parameters of low-pass filter circuit device are shown in Table I. The simulating analysis results obtained low-pass filter amplitude-frequency response shown in Fig. 4(b). As shown in Fig. 4, 3 dB cutoff frequency of 8.237 Hz meet the design requirements.

Table I. Selection of parameters of low-pass filter circuit component

component label	theoretical value	selection (nominal value)
C_1	≤250 nF	220 nF
C_3	≤45 nF	39 nF
R_1, R_2, R_3	33 K	33 K
R_4	17.982 K	18 K
R_5	179.82 K	180 K
R_6	36.083 K	36 K

Fig. 4(a) on the right is a high-pass (HP) filter circuit. The system used RC filter circuit and ratio phase amplifier to form a voltage-controlled voltage source second order high-pass filter, which has a high input impedance, low output impedance features. The transfer function Butterworth high-pass filter is

$$H(s) = \frac{K}{1 + (3 - K)\frac{1}{sRC} + \left(\frac{1}{sRC}\right)^2} \tag{11}$$

$$\omega_c = \frac{1}{RC} \tag{12}$$

$$K = 1 + \frac{R_9}{R_{10}} \tag{13}$$

Where K is the filter gain, ω_c is filter cutoff frequency.

According to design requirement, the cutoff frequency $f_c = 0.1\,\text{Hz}$, filter gain $K = 10$. When $f = 0.1 f_c$, the required amplitude attenuation is greater than 30 dB, so $R_7 = R_8 = R$, $C_5 = C_6 = C$, $f_c = 1/(2\pi RC)$. High-pass filter circuit component parameters as shown in Table II. Fig. 4(b) shows the simulating results for the voltage-controlled voltage source amplitude-frequency response of high-pass filter,

DOI: 10.1587/elex.14.20161178
Received November 28, 2016
Accepted December 16, 2016
Publicized January 18, 2017
Copyedited February 10, 2017

IEICE Electronics Express, Vol.14, No.3, 1–9

the 3 dB cutoff frequency of 0.099 Hz, the band-pass characteristics meet the design requirements.

Table II. High-pass filter circuit component parameter selection

component label	theoretical value	Selection nominal value
C_5, C_6	100 nF	100 nF
R_7, R_8	15.9 K	16 K
R_9	63.5 K	62 K
R_{10}	7.06 K	6.8 K

4 Algorithm of separation between respiration and heartbeat signals

The spectrum of respiration and heartbeat signals are located in two different frequency bands, both FIR and IIR filters were designed in the system for separating respiration and heartbeat signals [9, 10]. For the FIR filter, the signal of the frequency characteristics is simple to achieve linear phase, but the order of the filter is high, and the storing unit require much larger delay signal. While the IIR filter can achieve the same design specifications with smaller filter order, and require less computation storage unit etc., but it has a serious filtered signal phase distortion. In this system a two-direction filtering method was employed to achieve zero-phase shift, which can increase the amount of computation, completely eliminate of phase distortion signal.

According to the bands of respiration and heartbeat, parameter indexes to achieve the desired separation of the two signals of the filter are shown in Table III.

Table III. Parameters of digital signal separation filter

Physiological signal	f_s (sampling rate)	ω_s (band-pass cutoff frequency)	ω_p (stop-band cutoff frequency)	R_p (band-pass gain)	R_s (stop-band gain)
respiration	50 Hz	0.2 Hz	0.8 Hz	1 dB	40 dB
Heartbeat	50 Hz	0.8 Hz	4 Hz	1 dB	40 dB

Comparing to other types of filters, an ellipsoid IIR filter has the smallest oscillation at both pass-band and stop-band at the same order conditions, then used Matlab signal processing toolbox to estimate the order of ellipsoid function, it invokes formula

$$\Omega_p = \frac{2\pi}{\omega_p} \tag{14}$$

$$\Omega_s = \frac{2\pi}{\omega_s} \tag{15}$$

$$[N, \Omega_p] = ellipord(\Omega_p, \Omega_s, R_p, R_s) \tag{16}$$

DOI: 10.1587/elex.14.20161178
Received November 28, 2016
Accepted December 16, 2016
Publicized January 18, 2017
Copyedited February 10, 2017

Under the same design specifications, equation (14–16) can be calculated respiration and heartbeat signal of a desired signal elliptic filter order N 8 and 14, respectively.

The basic principle of zero-phase digital filter is a so-called two-direction filtering processing [10, 11]. The original signal is first flitted from the start, and the same filter is then applied to the flitted signal from the end, as if it backwards to filter the signal. The filtering result of zero phase shift, and zero-phase digital filter time-domain implementation process as defined in formula

$$y_1(n) = x(N-1-n) \tag{17}$$

$$y_2(n) = y_1(n) * h(n) \tag{18}$$

$$y_3(n) = y_2(N-1-n) \tag{19}$$

$$y(n) = y_3(n) * h(n) \tag{20}$$

Where in, $x(n)$ is the original signal sample sequence, N is the length of the signal sequence, $h(n)$ is digital filter impulse response sequence, $y(n)$ is zero phase filter output sequence. Of the formula (17–20) Fourier transform the frequency domain expression is available

$$Y_1(e^{j\omega}) = X(e^{j\omega})H(e^{j\omega}) \tag{21}$$

$$Y_2(e^{j\omega}) = e^{-j\omega(N-1)}Y_1(e^{-j\omega}) \tag{22}$$

$$Y_3(e^{j\omega}) = Y_2(e^{j\omega})H(e^{j\omega}) \tag{23}$$

$$Y_4(e^{j\omega}) = e^{-j\omega(N-1)}Y_3(e^{-j\omega}) \tag{24}$$

By the formula (21–24) can be obtained, the final input-output relationship

$$Y(e^{j\omega}) = X(e^{j\omega})|H(e^{j\omega})|^2 \tag{25}$$

By the formula (25) can be obtained after the zero-phase filtering the input signal. The output signal is a function of the square of the filter multiplied. Filter output signal amplitude is reduced and eliminated phase distortion. According to the physiological signal filter design specifications, the Elliptic filter should be designed band-pass small, steep transition zone, stop-band attenuation fast and so on. The system uses an elliptic filter configured zero phase filter. Fig. 2 shows physiological signal separation results using zero-phase IIR filter.

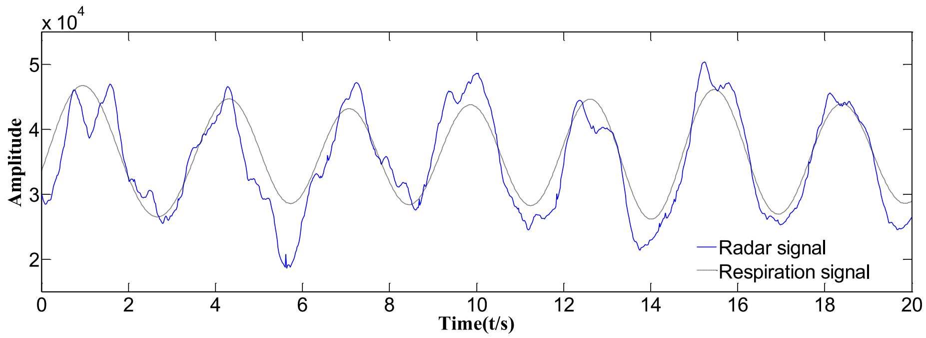

(a) Radar signal and the respiration signal filtered by zero-phase IIR

© IEICE 2017
DOI: 10.1587/elex.14.20161178
Received November 28, 2016
Accepted December 16, 2016
Publicized January 18, 2017
Copyedited February 10, 2017

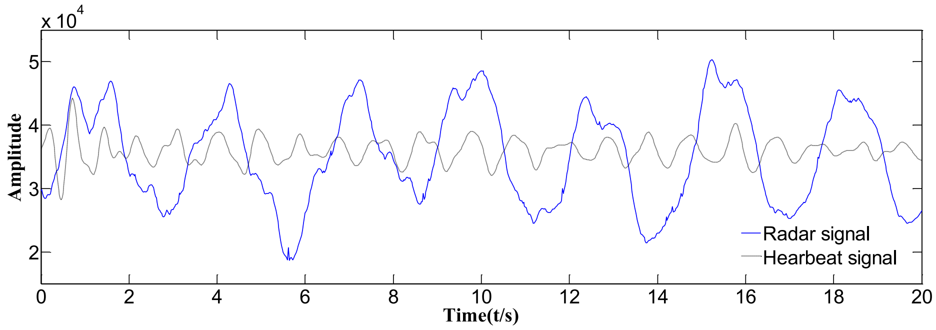

(b) Radar signal and the heartbeat signal filtered by zero-phase IIR

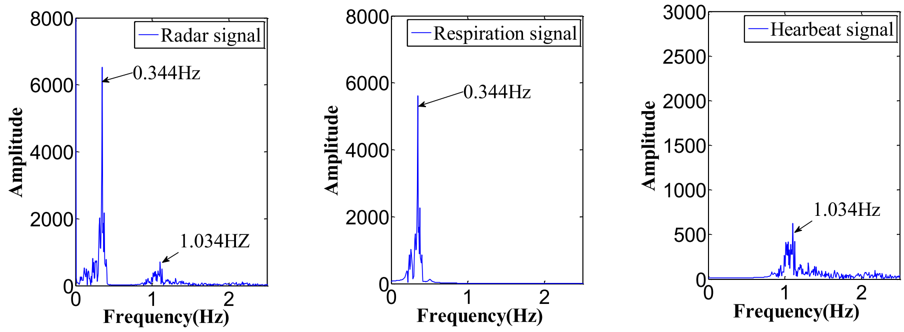

(c) Spectrum for radar signal, respiration signal, and heartbeat signal

Fig. 5. Results of zero-phase IIR filter for extracting physiological signal from radar signal

As shown in Fig. 5(a–c), zero-phase IIR filter can successfully extract both respiration and heartbeat signals from obtained Doppler radar signal after the signal spectrum has a single frequency. Comparing with the extracted respiration signal analysis, the optimized filter design and original phase signal phase breathing protection consistent, improving the initial portion of the waveform distortion, phase distortion is eliminated.

5 Conclusion

The Doppler radar signal acquisition system using a zero phase IIR filter for separating respiration and heartbeat signals can reduce the amount of computation, eliminate the signal phase distortion, ensuring signal integrity and improve the accuracy and reliability of detection. This non-contact physiological signal monitoring system could be potentially applied for detection of patients in hospital, such as patients with large area burns, skin ulceration or sleep disorders. The system could also be used in the field of earthquake, landslides and other disasters.

Acknowledgments

This work was supported in part by the Zhejiang provincial Science & Technology Innovation Team focused fund (Grant No. 2013TD03), the Key Laboratory of Solid State Disk and Data security of Zhejiang Province (Grant No. 2015E10003), and the Scientific Research Fund of Zhejiang Provincial Education Department (No. Y200701938).

DOI: 10.1587/elex.14.20161178
Received November 28, 2016
Accepted December 16, 2016
Publicized January 18, 2017
Copyedited February 10, 2017